Geometrical birefringence in square-lattice holey fibers having a core consisting of a multiple defect

Masashi Eguchi

Department of Applied Photonics System Technology, Chitose Institute of Science and Technology, Chitose, 066-8655 Japan

Yasuhide Tsuji

Department of Electric and Electronic Engineering, Kitami Institute of Technology, Kitami, 090-8507 Japan

Received July 24, 2006; revised November 14, 2006; accepted November 16, 2006; posted November 22, 2006 (Doc. ID 73320); published March 15, 2007

Geometrical birefringence in circular- and elliptical-hole square-lattice holey optical fibers having a core consisting of a multiple defect is investigated. The effect of unidirectional extension of the core area on the birefringence of these holey fibers (HFs) is discussed. We demonstrate that, as expected, a high birefringence can be induced in circular-hole HFs by unidirectional extension of the core area. In contrast, the maximum birefringence of elliptical-hole HFs, the holes of which have their major axes parallel to the long axis of the core, is achieved in a core structure that has a single defect. We also found that for elliptical holes having their major axes orthogonal to the long axis of the core, an exchange of the fast and slow modes occurs between the two orthogonally polarized fundamental modes by birefringence compensation.

OCIS codes: 060.2310, 060.2400, 060.2420.

1. INTRODUCTION

Photonic crystal fibers (PCFs), often referred to as microstructured fibers, are currently one of the most active research areas in the field of fiber optics. This is because PCFs exhibit a variety of unique guiding properties, including anomalous waveguide dispersion at short wavelengths,[1,2] large mode area,[3] high nonlinearity,[4,5] and endlessly single-mode behavior.[6] A PCF is a single-material optical fiber having a periodic pattern of air holes in the cladding and was developed by the authors of Ref. 7. The PCFs can be generally classified into two types according to their guidance mechanism. These are holey fibers (HFs) (frequently referred to as index-guiding fibers), in which light is guided by total internal reflection, and photonic bandgap fibers, in which light is guided by photonic bandgap effects. These HFs can also be made highly birefringent by using high index contrast, and various highly birefringent HFs have recently been proposed.[8–15] Highly birefringent fibers are attractive for their implementation in fiber-optic sensing systems, fiber devices, and coherent optical communication systems.[16] Birefringent circular-hole HFs having a core consisting of a multiple defect have already been reported. To our knowledge, however, there have been no systematic investigations of the geometrical birefringence of HFs having a core consisting of a multiple defect, including birefringence factors in such structures. In this paper we focus on index-guiding square-lattice HFs having a core consisting of a multiple defect. We investigate the effect of unidirectional extension of the core on the geometrical birefringence of the fiber and discuss the dominant factors that determine the birefringence in such structures. Although it is expected that the results for square-lattice fibers will be approximately similar to those for triangular-lattice fibers, we evaluate the square-lattice structure. This is because there have been no reports on square-lattice HFs having a core consisting of a multiple defect. Moreover, these structures are closer to planar (or rectangular) waveguides having high index contrast that have enhanced birefringence due to a large geometrical anisotropy. Recently a lamellar-core fiber having a very high birefringence, caused by artificially induced anisotropy in the core, has been fabricated.[17] The polarization properties of elliptical-hole square-lattice HFs having a core consisting of a single defect have already been reported,[18,19] and square-lattice HFs were fabricated in Ref. 20. So far, a variety of numerical approaches have been adopted to analyze HFs.[21] We use a finite-difference frequency-domain (FDFD) method[22,23] to obtain the dispersion properties of square-lattice HFs having a core consisting of a multiple defect. The FDFD method is a full-vector finite-difference mode solver that directly discretizes the Maxwell's equations by making use of Yee's mesh.[24] The validity of this approach for HFs was demonstrated in Ref. 22. In addition, in Ref. 22, the electric-wall boundary condition is used for the computation window edges, which are referred to as artificial or virtual boundaries. However, the boundary conditions on the artificial boundaries significantly affect the FDFD solutions in the low-frequency range. Therefore, we used an improved virtual-boundary method (IVBM)[25] to reduce the influence of these artificial boundaries. The IVBM imposes appropriate electric or

magnetic wall conditions on the virtual boundaries, which do not restrict the dominant components of each polarization mode there.

First, in Section 2, we demonstrate the polarization mode properties of circular- and elliptical-hole square-lattice HFs having a core consisting of a multiple defect, and we discuss the dominant factors that determine the birefringence in such structures. Section 3 is devoted to elliptical-hole HFs whose holes have their major axes aligned orthogonal to the long axis of the core.

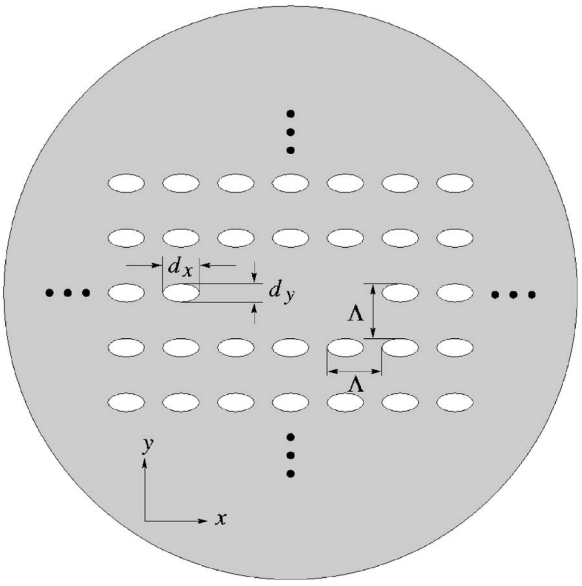

Fig. 1. Elliptical-hole square-lattice HF with a core consisting of a triple defect.

2. SQUARE-LATTICE HFs HAVING A CORE CONSISTING OF A MULTIPLE DEFECT

A. Circular Air Holes

In this section, we consider circular-hole square-lattice HFs having a core consisting of a multiple defect. The schematic design of our HFs is indicated in Fig. 1. The HF in Fig. 1 represents an elliptical-hole HF having a core consisting of a triple defect and is characterized by an ellipticity $\eta = d_y/d_x$, and a lattice pitch Λ. The refractive index of fused silica is 1.45. Figure 2 shows the birefringences predicted by theory for a series of circular-hole HFs, which correspond to $\eta = 1$ or $d_x = d_y$ in Fig. 1, having different hole sizes. Here, B represents the polarization modal birefringence of the two orthogonally polarized fundamental modes defined as the difference $(n_{eff,x} - n_{eff,y})$ in the effective index of the two modes, Λ/λ is the normalized frequency, and $\xi = d_x/\Lambda$. In the case of a circular-hole structure, the two orthogonally polarized modes in HFs having a core consisting of a single defect are degenerate. Figures 2(a)–2(d) correspond to cores consisting of double, triple, fourfold, and fivefold defects, respectively. The solid, dashed-dotted, and dashed curves in Fig. 2 denote hole sizes of $\xi = 0.7$, 0.5, and 0.3, respectively. The second-order cutoffs are indicated on the horizontal axes by arrows. The second-order cutoff represents the cutoff of the second-order mode (frequently referred to as the first higher-order mode) that has a high effective index next to the two orthogonally polarized fundamental modes, designated HE_{11}^x and HE_{11}^y in the Marcatili notation.[26] For the structures mentioned in this section, the second-order mode corresponds to the x-polarized HE_{21} mode. High birefringence is achieved at low frequencies (approximately $\lambda > \Lambda$), because light confinement becomes stronger as

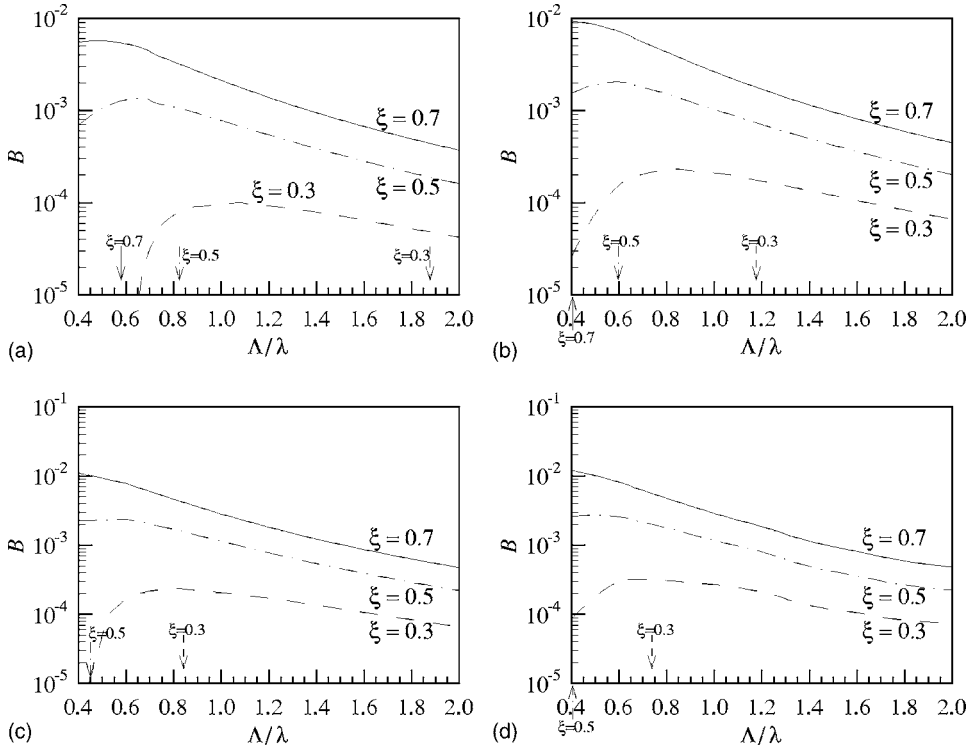

Fig. 2. Birefringence of circular-hole square-lattice HFs ($\eta = 1$) with cores consisting of (a) double, (b) triple, (c) fourfold, and (d) fivefold defects. The second-order cutoffs are marked on the horizontal-axes by arrows.

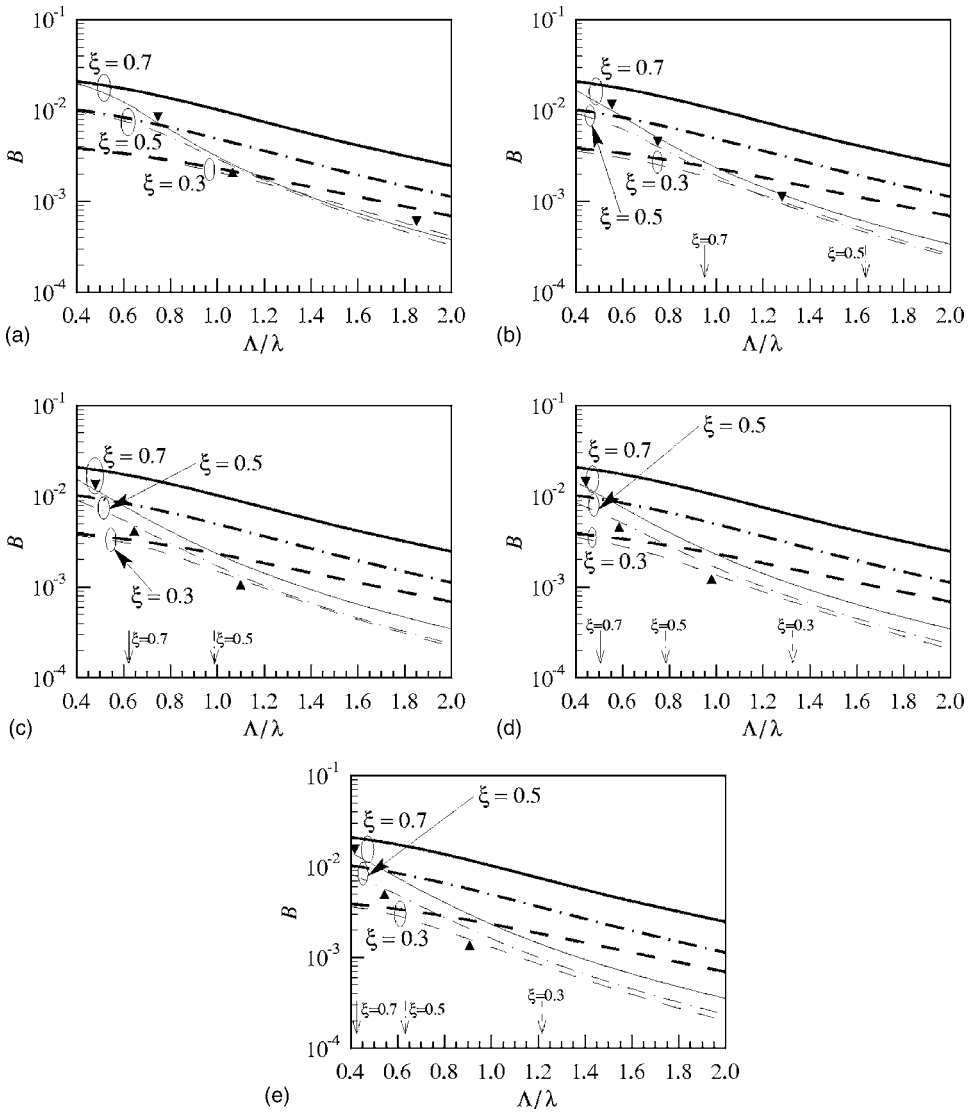

Fig. 3. Birefringence of elliptical-hole square-lattice HFs (η=0.5) with cores consisting of (a) single, (b) double, (c) triple, (d) fourfold, and (e) fivefold defects. In the frequency range until triangles, the y-polarized modes are leaky modes with respect to the x-polarized FSM. The second-order cutoffs are marked on the horizontal axes by arrows.

Λ/λ increases, reducing the effect of geometric anisotropy. In addition, the birefringence increases greatly with hole size.

B. Elliptical Air Holes with Their Major Axes Parallel to the Long Axis of the Core

Next, we discuss square-lattice HFs having elliptical air holes (η=0.5) the core shapes of which approach a planar shape with increasing ellipticity of the holes. Here the major axis of each hole is aligned along the x axis. The birefringences of elliptical-hole HFs having different hole sizes are shown in Fig. 3, and the solid, dashed-dotted, and dashed curves denote hole sizes of ξ=0.7, 0.5, and 0.3, respectively. Figures 3(a)–3(e) correspond to cores consisting of single, double, triple, fourfold, and fivefold defects, respectively. The thick curves in Fig. 3 denote the fundamental space-filling mode (FSM) birefringences for ξ =0.7, 0.5, and 0.3. The second-order cutoffs are indicated on the horizontal-axes by arrows. Additionally, the y-polarized modes are leaky modes with respect to the x-polarized FSM for frequencies less than those indicated by the triangles on the plot. At relatively low frequencies, the birefringence of elliptical-hole HFs results from the difference between the equivalent refractive-indices for the x- and y-polarized light in the cladding, which is referred to as the anisotropy, since the birefringence asymptotically approaches that of the FSM.

C. Discussion

As can be seen from Figs. 2 and 3, a high birefringence can be induced by unidirectional extension of the core area for circular-hole HFs, whereas the maximum birefringence of elliptical-hole HFs is achieved in a core structure consisting of a single defect. This is because the geometric anisotropy of the core area produces birefringence in circular-hole HFs. In elliptical-hole HFs, on the other hand, as mentioned above, the cladding that behaves as an anisotropic medium is the dominant factor of birefringence, and the extension of the field into the cladding produces high birefringence. For the same reason, it is pre-

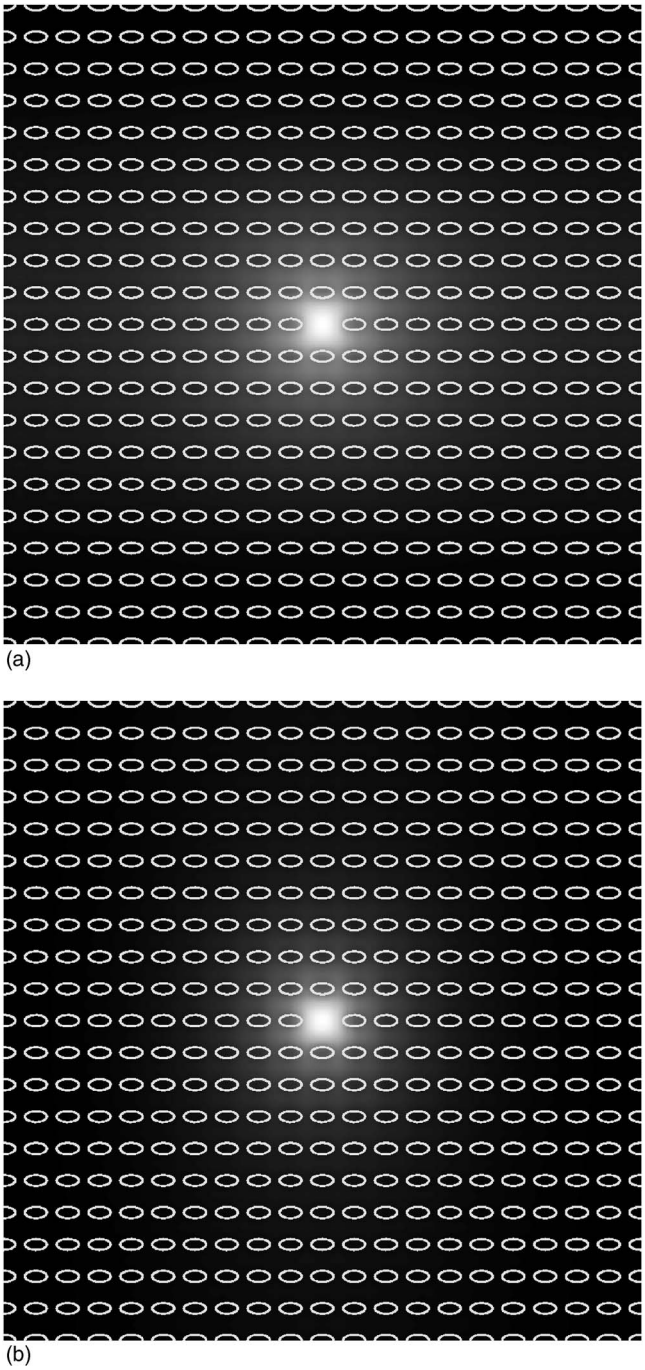

Fig. 4. Intensity distributions of dominant component in the (a) x- and (b) y-polarized modes for the elliptical-hole HF ($\xi=0.7$) with a core consisting of a single defect at $\Lambda/\lambda=0.4$.

dicted that the birefringence of circular-hole HFs is strongly influenced by hole size compared with that of elliptical-hole HFs. Additionally, we observed that, in the case of a core consisting of a single defect, the birefringence for a hole size of $\xi=0.3$ [the dashed curve in Fig. 3(a)] exceeds that for $\xi=0.7$ (the solid curve) as Λ/λ increases. The reason for this is that, for low Λ/λ the field penetrates deeply into the cladding, so that a cladding having large elliptical holes ($\xi=0.7$) produces large anisotropies. By contrast, for high Λ/λ the light confinement becomes strong and the light propagating in a HF having small holes ($\xi=0.3$), whose light confinement is weaker than that of a HF with large holes, is affected by the anisotropy of the cladding more strongly.

The mode field becomes highly elliptical when multiple defects are introduced. This would be incompatible with standard fibers, which have a circular mode field, in terms of splice loss. Fortunately, however, the maximum birefringence of elliptical-hole HFs occurs when their mode fields are comparable with those of standard fibers, e.g., in single-defect cores. It can also be noticed that the second-order cutoff of elliptical-hole HFs shifts toward high frequency compared with that of circular-hole HFs. This shift extends the single-mode operation range so that high birefringence of fundamental mode is realized in the single mode operation region, as seen from Fig. 3.

Figures 4(a) and 4(b) show the intensity distributions of the dominant components of the x- and y-polarized fundamental modes, respectively, for an elliptical-hole HF, which results in a maximum birefringence. The HF has a core consisting of a single defect and corresponds to the solid curve at $\Lambda/\lambda=0.4$ in Fig. 3(a). A difference in the penetration of the field into the anisotropic cladding is observed between the two polarized modes.

In the low frequency range, HFs having even- and odd-fold defects exhibit different properties. This is particularly remarkable for HFs having small circular holes ($\xi=0.3$), as seen from Fig. 2. There are no holes in the y direction of the core center, where the peak of the mode field of the fundamental mode is located, for HFs having even-fold defects. In the low frequency range, when the hole size is reduced, it functions as a thin slab waveguide. The slab waveguide, which includes a defect area, produces properties that resemble those of a rib waveguide weakly, in which the y-polarized mode is dominant. This effect cancels out the birefringence produced by core asymmetry

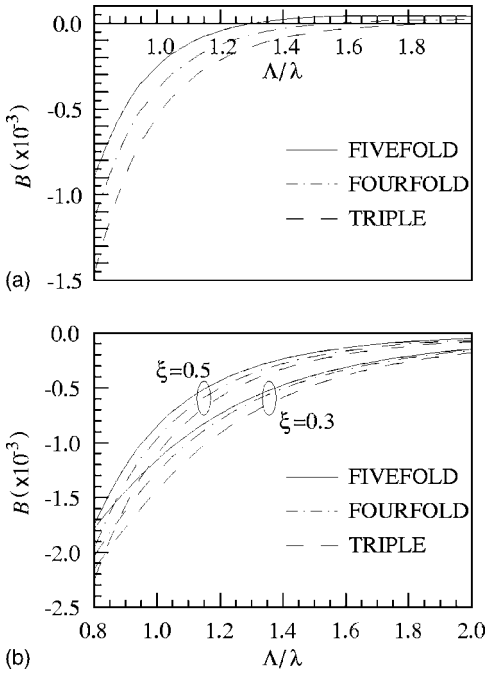

Fig. 5. Birefringence of elliptical-hole square-lattice HFs ($\eta=2$) with cores consisting of triple, fourfold, and fivefold defects. (a) $\xi=0.7$. (b) $\xi=0.5$ and 0.3.

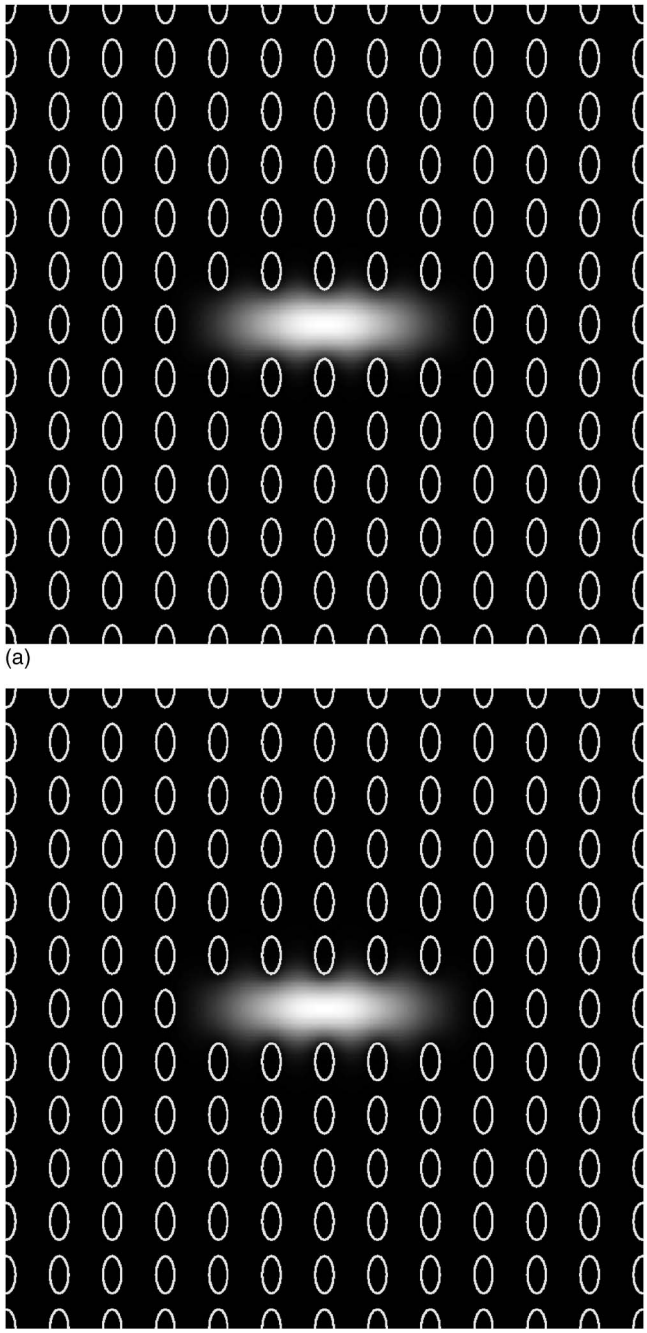

Fig. 6. Intensity distributions of dominant component in the (a) x- and (b) y-polarized modes for the elliptical-hole HF ($\xi=0.7$) with a core consisting of a fivefold defect at $\Lambda/\lambda=1.3046$.

with the x-polarized mode being the dominant mode and, in the low frequency range, the birefringence of circular-hole HFs having small holes decreases rapidly for even-fold defects, as shown in Fig. 2.

3. HOLEY FIBERS HAVING ELLIPTICAL AIR HOLES WHOSE MAJOR AXES ARE ORTHOGONAL TO THE LONG AXIS OF THE CORE

Finally, we examine the birefringence of HFs having elliptical air holes ($\eta=2$) whose major axes are parallel to the y axis. The calculated birefringences for HFs with $\xi=0.7$, and 0.5 and 0.3 are illustrated in Figs. 5(a) and 5(b), respectively. In Fig. 5, the solid, dashed-dotted, and dashed curves denote cores consisting of fivefold, fourfold, and triple defects, respectively. In these structures, the geometric anisotropies of core and cladding areas, which are two factors that exert a strong influence on the birefringence, tend to cancel each other out. As a result, the birefringence of these HFs decreases drastically with increasing Λ/λ and eventually becomes positive. This means that an exchange of the fast and slow modes occurs between the two orthogonally polarized fundamental modes by birefringence compensation when the elliptical holes have their major axes aligned orthogonal to the long axis of the core.

Figures 6(a) and 6(b) show the intensity distributions of the dominant component in the x- and y-polarized fundamental modes, respectively, for a HF that has $B=0$. The HF has a core consisting of a fivefold defect ($\xi=0.7$) and corresponds to the solid curve at $\Lambda/\lambda=1.3046$ in Fig. 5(a). The two polarization modes have similar intensity distributions and the light is tightly confined within their core regions.

4. CONCLUSION

We have investigated the effect of unidirectional extension of the core area on the polarization mode properties of square-lattice HFs by using the FDFD method. Our analysis reveals that unidirectional extension of the core is effective in increasing the birefringence for circular-hole HFs, but it is not effective for elliptical-hole HFs. This implies that the anisotropy of cladding is the dominant factor for producing birefringence in elliptical-hole HFs whose holes have their major axes aligned parallel to the long axis of the core. Furthermore, for elliptical holes having their major axes orthogonal to the long axis of the core, we found an exchange of the fast and slow modes occurs between the two orthogonally polarized fundamental modes by birefringence compensation.

In this paper, we have focused on the geometrical birefringence of HFs. However, group velocity walk-off and chromatic dispersion are other important characteristics in birefringent fibers that need to be considered. We intend to investigate these characteristics in the future.

ACKNOWLEDGMENTS

The authors thank T. Nagai for his excellent cooperation on the computer system.

M. Eguchi's e-mail address is megu@paical.spub.chitose.ac.jp, and Y. Tsuji's e-mail address is tsujiya@mail.kitami-it.ac.jp.

References

1. M. Gander, R. McBirde, J. Jones, D. Mogilevtsev, T. Birks, J. Knight, and P. Russell, "Experimental measurement of group velocity dispersion in photonic crystal fibre," Electron. Lett. **35**, 63–43 (1999).
2. J. C. Knight, J. Arriaga, T. A. Birks, A. Ortigosa-Blanch, W. J. Wadsworth, and P. St. J. Russell, "Anomalous dispersion

in photonic crystal fiber," IEEE Photon. Technol. Lett. **12**, 807–809 (2000).
3. J. C. Knight, T. A. Birks, R. F. Cregan, P. St. J. Russell, and J.-P. De Sandro, "Large mode area photonic crystal fibre," Electron. Lett. **34**, 1347–1348 (1998).
4. J. K. Ranka, R. S. Windeler, and A. J. Stentz, "Optical properties of high-delta air-silica microstructure optical fibers," Opt. Lett. **25**, 796–798 (2000).
5. P. Petropoulos, T. M. Monro, W. Belardi, K. Furusawa, J. H. Lee, and D. J. Richardson, "2R-regenerative all-optical switch based on a highly nonlinear holey fiber," Opt. Lett. **26**, 1233–1235 (2001).
6. T. A. Birks, J. C. Knight, and P. St. J. Russell, "Endlessly single-mode photonic crystal fiber," Opt. Lett. **22**, 961–963 (1997).
7. J. C. Knight, T. A. Birks, P. St. J. Russell, and D. M. Atkin, "All-silica single-mode optical fiber with photonic crystal cladding," Opt. Lett. **21**, 1547–1549 (1996).
8. A. Ortigosa-Blanch, J. C. Knight, W. J. Wadsworth, J. Arriaga, B. J. Mangan, T. A. Birks, and P. St. J. Russell, "Highly birefringent photonic crystal fibers," Opt. Lett. **25**, 1325–1327 (2000).
9. M. J. Steel and R. M. Osgood, Jr., "Elliptical-hole photonic crystal fibers," Opt. Lett. **26**, 229–231 (2001).
10. M. J. Steel and R. M. Osgood, Jr., "Polarization and dispersive properties of elliptical-hole photonic crystal fibers," J. Lightwave Technol. **19**, 495–503 (2001).
11. K. Suzuki, H. Kubota, S. Kawanishi, M. Tanaka, and M. Fujita, "Optical properties of a low-loss polarization-maintaining photonic crystal fiber," Opt. Express **9**, 676–680 (2001).
12. T. P. Hansen, J. Broeng, S. E. B. Libori, E. Knudsen, A. Bjarklev, J. R. Jensen, and H. Simonsen, "Highly birefringent index-guiding photonic crystal fibers," IEEE Photon. Technol. Lett. **13**, 588–590 (2001).
13. P. R. Chaudhuri, V. Paulose, C. Zhao, and C. Lu, "Near-elliptic core polarization-maintaining photonic crystal fiber: modeling birefringence characteristics and realization," IEEE Photon. Technol. Lett. **16**, 1301–1303 (2004).
14. N. A. Issa, M. A. van Eijkelenborg, M. Fellew, F. Cox, G. Henry, and M. C. J. Large, "Fabrication and study of microstructured optical fibers with elliptical holes," Opt. Lett. **29**, 1336–1338 (2004).
15. M. Szpulak, G. Statkiewicz, J. Olszewski, T. Martynkien, W. Urbańczyk, J. Wójcik, M. Makara, J. Klimek, T. Naslilowski, F. Berghmans, and H. Thienpont, "Experimental and theoretical investigations of birefringent holey fibers with a triple defect," Appl. Opt. **44**, 2652–2658 (2005).
16. J. Noda, K. Okamoto, and Y. Sasaki, "Polarization-maintaining fibers and their applications," J. Lightwave Technol. **LT-4**, 1071–1089 (1986).
17. A. Wang, A. K. George, J. F. Liu, and J. C. Knight, "Highly birefringent lamellar core fiber," Opt. Express **13**, 5988–5993 (2005).
18. M. Y. Chen and R. J. Yu, "Polarization properties of elliptical-hole rectangular lattice photonic crystal fibers," J. Opt. A, Pure Appl. Opt. **6**, 512–515 (2004).
19. Y. C. Liu and Y. Lai, "Optical birefringence and polarization dependent loss of square- and rectangular-lattice holey fibers with elliptical air holes: numerical analysis," Opt. Express **13**, 225–235 (2005).
20. P. St. J. Russell, E. Marin, A. Díez, S. Guenneau, and A. B. Movchan, "Sonic band gaps in PCF preforms: enhancing the interaction of sound and light," Opt. Express **11**, 2555–2560 (2003).
21. A. Bjarklev, J. Broeng, and A. S. Bjarklev, *Photonic Crystal Fibres* (Kluwer Academic Publishers, 2003).
22. Z. Zhu and T. G. Brown, "Full-vectorial finite-difference analysis of microstructured fibers," Opt. Express **10**, 853–864 (2002).
23. S. Guo, F. Wu, S. Albin, H. Tai, and R. S. Rogowski, "Loss and dispersion analysis of microstructured fibers by finite-difference method," Opt. Express **12**, 3341–3352 (2004).
24. K. S. Yee, "Numerical solution of initial boundary value problems involving Maxwell's equations in isotropic media," IEEE Trans. Antennas Propag. **AP-14**, 302–307 (1966).
25. K. Hayata, M. Eguchi, M. Koshiba, and M. Suzuki, "Vectorial wave analysis of side-tunnel type polarization-maintaining optical fibers by variational finite elements," J. Lightwave Technol. **LT-4**, 1090–1096 (1986).
26. E. A. J. Marcatili, "Dielectric rectangular waveguide and directional coupler for integrated optics," Bell Syst. Tech. J. **48**, 2071–2102 (1968).